Processing and Application of Ceramics 14 [1] (2020) 1–8
https://doi.org/10.2298/PAC2001001Z

Microstructure and mechanical properties of Al_2O_3-Cu-Ni hybrid composites fabricated by slip casting

Justyna Zygmuntowicz[1,*], Paweł Falkowski[2], Marcin Wachowski[3], Aleksandra Miazga[1], Paulina Piotrkiewicz[1], Waldemar Kaszuwara[1]

[1]*Warsaw University of Technology, Faculty of Materials Science and Engineering, 141 Woloska Str., 02-507 Warsaw, Poland*
[2]*Warsaw University of Technology, Faculty of Chemistry, 3 Noakowskiego Str, 00-664 Warsaw, Poland*
[3]*Military University of Technology, Faculty of Mechanical Engineering, gen. W. Kaliskiego 2 Str., 00-908 Warsaw, Poland*

Received 20 August 2019; Received in revised form 8 November 2019; Accepted 23 December 2019

Abstract

This work focuses on developing the fabrication method of hybrid composites based on Al_2O_3-Cu system with the addition of nickel phase. The composites were prepared by slip casting and the slurries with a high concentration of solid content were used. The sintered composites were characterized by XRD, SEM and EDX. Selected physical proprieties, namely hardness, fracture toughness and bending strength were also determined. The microstructure and its influence on the mechanical properties were investigated. XRD analyses revealed that the obtained composites contained Al_2O_3, Ni, Cu and solid solution CuNi phases. The use of slip casting method allowed the production of the composites characterized by relative density of ~96%. An increase in metallic phase concentration caused a decrease in Vickers hardness and increased the fracture toughness of the Al_2O_3-Cu-Ni materials compared to the Al_2O_3 samples. The results with high cognitive value and application potential were obtained. This research enabled the foundations of an innovative method of forming hybrid composite structures, which combined the best features of ceramics (hardness, resistance to high temperature) with metal properties (crack resistance, good electrical conductivity). This type of composite can be used for temperature, conductivity and flow sensors.

Keywords: *Al_2O_3, Ni, Cu composites, slip casting, microstructure, mechanical properties*

I. Introduction

Composites are materials made of at least two different components, often characterized by very different properties [1]. Selection of proper materials as composite components with specific form, size and arrangement enables to obtain composites with better mechanical properties in comparison to the single-phase materials. This also provides an extended opportunity for thoughtful development of the required material properties [2]. Moreover, this gives the possibility to produce dedicated materials for a specific application. Composites are used in automotive and aerospace industries, in machining as a material for cutting tools and for biomaterials applications because of their promising features such as high hardness, amazing wear resistance and sensible chemical stability. Composites are also used in many different applications due to the connection of their high strength and hardness [1,3–7]. The review of specialist literature on ceramic-metal composites fabricated using the Pulse Plasma Sintering (PPS) technique shows that they are widely used in the electronics industry, e.g. as chip substrates, multilayer capacitors, fuel cells or plate electrodes [8]. Ceramic matrix composites are a group of materials that have attracted attention recently. High hardness, chemical resistance and stable mechanical properties at high temperatures cause that many works are devoted to them. Interesting research on these ceramic materials was conducted by Kafkaslioğlu Yildiz *et al*. [9]. The addition of the second ductile component improves the typical disadvantages of ceramics:

*Corresponding author: tel: +48 22 2348138,
e-mail: *Justyna.zygmuntowicz@pw.edu.pl*

brittleness and low thermal conductivity [10,11]. One of the predominantly effective techniques to increase fracture toughness of monolithic ceramics is its reinforcement by the addition of ductile metal particles. The metal particles interact with the prior or/and new cracks to slow down their extension [12–16].

In recent years, a new remarkable group of composites are hybrid composites, where phase structure is ultimately formed in the high-temperature consolidation process, as a result of the reaction such as phase transformation between the components [16]. Introduction of two reinforcing components, for example two metal powders into a ceramic matrix can produce new phases that change the properties of the composite. The aims of this study are to obtain Al_2O_3-Cu-Ni composites using slip casting method and characterize their microstructure and mechanical properties. The added nickel may improve the wettability of the metal phase during the fabrication of these type composites. There are no reports in the literature about the research on this type of system. Obtained results will gain new knowledge about the correlation between parameters of the production process, structure and selected properties of the composites made of the Al_2O_3-Cu-Ni.

II. Experimental procedure

The commercial α-Al_2O_3 TM-DAR (Tamei Chemicals Co., Japan) with a chemical purity of 99.99% was used as a ceramic powder. The morphology and particle size distribution of α-Al_2O_3 powder are presented in Fig. 1. Based on SEM images, it was found that the starting ceramic powder has a spherical shape, with an average equivalent diameter of 143.3 ± 55 nm. Furthermore, the microscopic observation revealed that the alumina powder shows a tendency to create agglomerates. The composite samples were prepared with the commercial metallic powders Ni (Bimo Tech, Poland) and Cu (Sigma-Aldrich, Poland). Particle size distribution (PSD) of the metal particles was determined by laser diffraction technique with the use of an Analyzer LA 950 Horiba. PSD analysis showed that Ni and Cu powders were characterized by an average particle size of 25 ± 15 μm and 13.34 ± 4.7 μm, respectively. Figure 2 shows morphology and XRD diffraction of metal powders used in the experiment. The SEM images of the metallic powders showed that the used Ni particles are characterized by irregular morphology, while the copper powder has mostly a regular spherical shape. The densities of the raw powders were measured by a helium pycnometer, AccuPyc II 1340 (Micromeritics), in a sequence of 100 purges and 100 measurement cycles. The conducted measurements showed that Al_2O_3 had a density of 3.94 g/cm^3, while Ni and Cu were characterized by a density equal to 8.90 and 8.94 g/cm^3, respectively.

To prepare a stable slurry with appropriate rheological properties made of Al_2O_3, Ni and Cu, Duramax-D3005 was used as dispersant in an amount of 1.5 wt.% with respect to the dry mass of the powders. Duramax-D3005 is the ammonium salt of a polyelectrolyte, helpful in dispersing a variety of ceramic and ceramic/metal powders in distilled water [18]. In the present work, slurry with 50 vol.% of solid content was obtained. A total metal share in this three-component system was 15 vol.%, wherein 7.5 vol.% was occupied by Cu and 7.5 vol.% by Ni. As a solvent ultra-pure Mili-Q water with conductivity below 9 mS/cm was used.

The Al_2O_3-Cu-Ni composites were fabricated with slip casting method. Firstly, powder mixtures with the

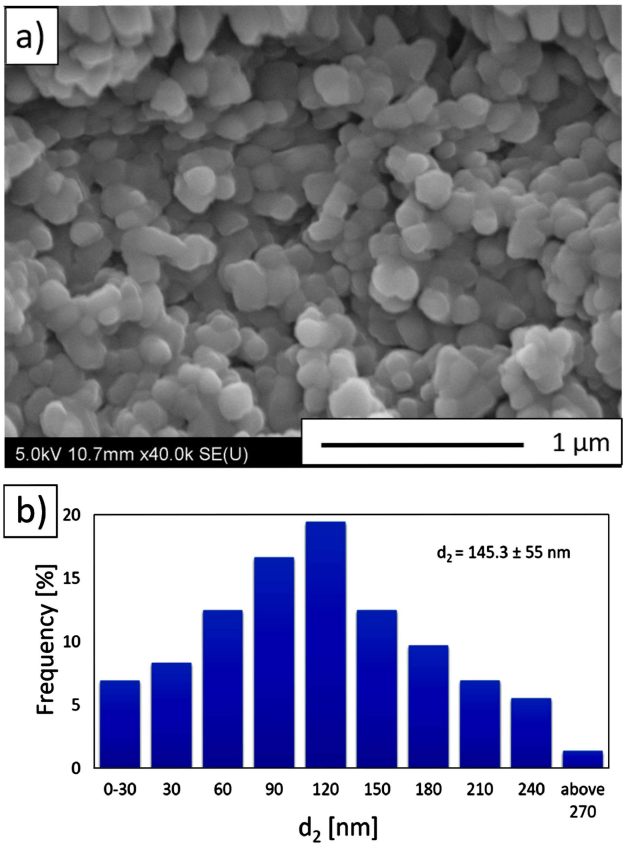

Figure 1. Morphology (a) and particle size distribution (b) of α-Al_2O_3 powder

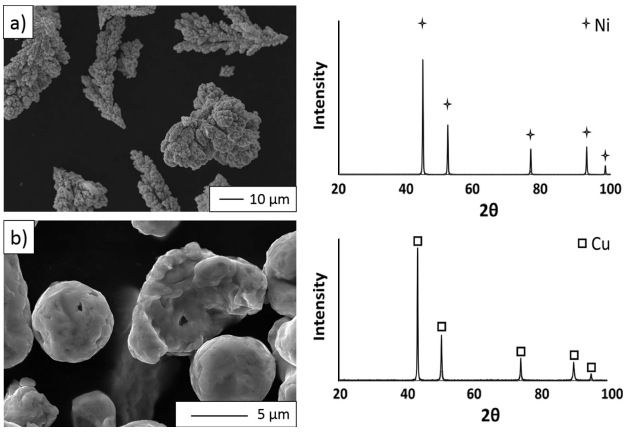

Figure 2. Morphology and diffraction of metal powders: a) Ni and b) Cu

following composition: Al_2O_3 85 vol.% - Cu 7.5 vol.% - Ni 7.5 vol.% were mixed in water along with Duramax. The addition of 1.5 wt.% of the dispersing agent allows to obtain the slurries which are flowable and stable over time. Composite slurry was ball milled in an alumina container for 60 min with a speed of 300 rpm. Furthermore, in order to remove air bubbles from suspension, slurries were additionally mixed and degassed in the Thinky ARE-250 Mixer and Degassing Machine for 5 min at 1800 rpm. Green samples were produced by slip casting the slurries into gypsum moulds followed by drying for 24 h at 40 °C in a vacuum oven. Subsequently, the densification of the composite was performed at 1400 °C in a gas flow which ensured reducing atmosphere (80% N_2 and balance H_2) with dwell time of 2 h. The reducing atmosphere was chosen to avoid oxidation of the metallic particles during the sintering process. The heating and cooling rates during the densification were 2 °C/min.

The zeta potential of the pure alumina, copper and nickel powders was measured using Zetasizer Nano ZS (Malvern Instruments Ltd). Measurements were made for 0.01 vol.% of colloidal dispersions in 10 mM NaCl solution. Before the measurements, every specimen was sonicated for 7 min in ultrasonic bath EMMI 12HC (EMAG). The pH of colloidal dispersions was controlled by addition of 0.1 M or 0.05 M solutions of HCl and NaOH, respectively. The density of sintered bodies was determined by the Archimedes method. For this measurements the true density of Al_2O_3-Cu-Ni composite bodies were calculated using the rule of mixture. The XRD analysis was accomplished to determine the bulk crystalline phases of the Al_2O_3-Cu-Ni materials. It was conducted using a Rigaku MiniFlex II diffractometer using CuK_α radiation (λ = 1.54178Å). The XRD conditions of recording were as follows: voltage 30 kV, current 15 mA, angular range 2θ 20°–100°, step 0.02° and counting time 3 s on the cross section of the specimen. The measurements were performed at ambient temperature.

The observation of the cross section and fracture of the composite samples was performed using a scanning electron microscope JEOL JSM-6610 with backscattered electrons (BSE) and energy-dispersive X-ray spectroscopy (EDX) detectors. SEM images in BSE mode were obtained at acceleration voltage of 10 kV. EDX chemical composition analyses of the samples were performed at acceleration voltage of 15 kV. Cross section of the composite was prepared by SiC papers grinding and polishing using 3 μm and 1 μm diamond suspension. For high resolution SEM observation the polished samples were finally carbon coated using Quorum Q150T ES Coating system.

Quantitative description of the microstructure was made on the basis of SEM images of randomly selected areas on the specimens using computer image analysis applying the program Micrometer [19]. This procedure allows obtaining data about the actual size and distribution of metallic phases in the composites. The all metal particles were characterized by parameter d_2 - diameter of circle of the same surface as the surface of the investigated grain. Based on the scores of image analysis, the average values of shape factors describing metal particles have been determined as following: surface development ($R = p/(\pi \cdot d_2)$), elongation ($\alpha = d_{max}/d_2$) and convexity ($W = p/p_C$), where p is perimeter of particle, d_{max} is maximum diameter of particle projection and p_C is Cauchy perimeter [19].

The hardness and fracture toughness were measured with a Vickers Hardness Tester (WPM LEIPZIG HPO-250) using the indentation technique under the load of 196 N with 15 s holding time. Fifteen indentations were made for five samples. The measurements of the diagonals and cracks have been done on the HITACHI TM-1000 scanning electron microscope. The fracture toughness has been calculated based on two formulas [20–24], the Niihara equation for $0.25 < l/c < 2.5$:

$$K_{IC} = 0.018 \cdot HV^{0.6} \cdot E^{0.4} \cdot 0.5d \cdot l^{-0.5} \tag{1}$$

and the Anstis equation for $l/a > 1.5$:

$$K_{IC} = 0.016\left(\frac{E}{HV}\right)^{0.5} \cdot \frac{P}{c^{1.5}} \tag{2}$$

where HV is Vickers hardness, E is Young's modulus, d is diagonal of the Vickers indentations, l is average crack length, P is indentation load and c is crack length from the centre of the indentation to the crack tip.

In this work, a mechanical strength was determined by a Brazilian test [25,26], which is indirect tensile strength measurement method. The procedure implies the diametrical compression of a disk of material, which produces a tensile stress state in the specimen which is maximum and constant along the diameter coincident with the loading direction, so the failure occurs along this direction. The tensile stress can be derived from the following equation [25,26]:

$$\sigma_0 = \frac{2F}{\pi \cdot D \cdot t} \tag{3}$$

where F is the value of the applied load and D and t are, respectively, the diameter and the thickness of the specimen.

III. Results and discussion

Figure 3 shows the measured zeta potential profiles of the alumina, Ni and Cu dispersions versus pH. The zeta potential values of the alumina and copper dispersions with addition of dispersant are also reported. In the present work, as the pH was increasing from 2 to 12, the zeta potential of the alumina suspension was decreasing from 45 to −41 mV with isoelectric point (IEP) around 9. The dispersant (Duramax) was found to affect the zeta potential changes of the suspension with alu-

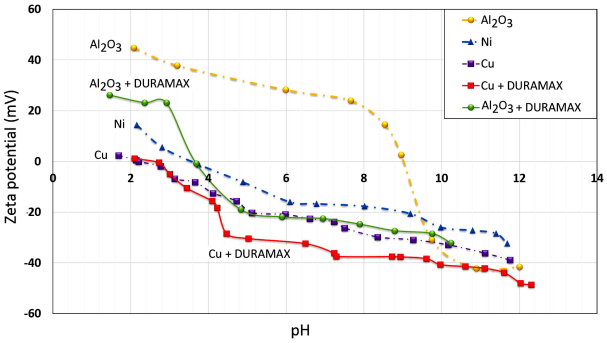

Figure 3. Zeta potential of Al_2O_3, Ni and Cu with and without dispersing agent

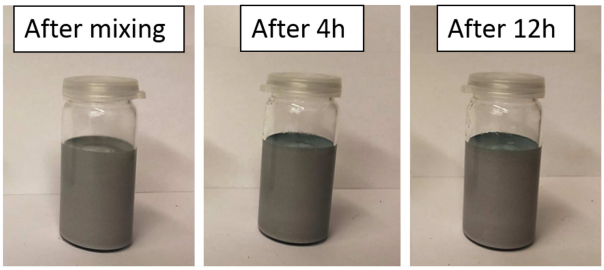

Figure 4. Composite slurries after mixing as well as after 4 and 12 hours from mixing

mina. Thus, the IEP of slurry with TM-DAR is shifted to 3.8. In the case of the metal powders the presence of dispersing agent did not shift the IEP, but increasing of the absolute value of zeta potential above −30 mV in the pH range 5–12 was observed for the Cu suspensions. Direct measurements allowed us to observe that the final ceramic suspension, used for slip casting, had a pH around 8.5. Thus, at these conditions the alumina and metal particles carry the same negative and high surface charge which gives good stability of obtained suspensions in time.

In order to confirm the stability of the slurries over time, observations of the obtained suspensions were carried out for 12 h from the moment of their mixing (Fig. 4). The slurry was placed in glass container and the photos were taken every two hours. During the test time no sedimentation was observed and even after 12 h the suspension was stable and no phase separation was observed. Due to the lack of sedimentation of the metal particles in the suspensions, the distribution of the metallic phase was expected to be homogeneous in the green samples.

The Archimedes measurements demonstrated that all sintered samples had a relative density of over 96% TD and open porosity equal to 0.45%. It can be noticed that the samples are described by the linear shrinkage equal to 13.3%. However, the volume shrinkage was 35.3%.

The phase composition of the obtained composite is shown in Fig. 5. The XRD patterns reveal four phases: Al_2O_3, Ni, Cu and CuNi solid solution (characterized by the cubic structure, $Fd\bar{3}m$). The characteristic peaks at 43.97°, 51.22°, 75.37°, 91.59° and 96.96° in CuNi correspond to the plane indices (111), (200), (220), (311) and (222), respectively (ICDD 04-003-7260). There was no nickel aluminate spinel phase ($NiAl_2O_4$) not copper aluminate spinel ($CuAl_2O_4$) in the composites after sintering. The absence of the spinel phase peaks indicates that nickel and cooper have not reacted with alumina. This research has shown that the use of a reducing atmosphere allowed avoiding the appearance of spinel phases in the composite materials.

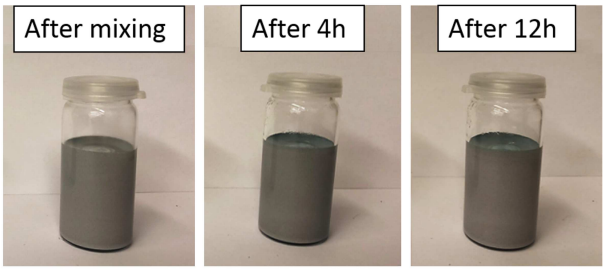

Figure 5. XRD patterns of Al_2O_3-Ni-Cu composite sintered at 1400 °C

Based on the obtained SEM images (Fig. 6) in BSE mode (where light areas represent nickel/copper particles while dark represent Al_2O_3) and microstructural analysis, it was stated that distribution of metallic particles in the matrix is homogenous with the tendency for agglomeration. SEM observation of the cross section of the composite revealed the presence of pores and voids in the structure. However, cracks were not observed. EDX distribution of the elements on the surface of sample confirmed chemical composition of the light and dark areas in SEM images as CuNi solid solution and Al_2O_3, respectively (Fig. 7). Additionally, elemental maps observations revealed that no interlayer or spinel is present between metallic phase and matrix.

The existence of new CuNi phase and small porosity in the sintered samples are probably due to the low melting temperature of Cu and low wettability of the alumina surface by the molten metal. At Cu melting temperature (1085 °C) the densification of alumina matrix is just starting, thus the samples are very porous. Due to the higher surface tension of molten Cu (1240 mN/m at 1400 °C) in respect to the surface energy of alumina (sapphire, 700 mJ/m^2 at 2080 °C) the molten copper does not wet the alumina surface. Normally it causes that the molten copper is leaking out through the open pores. However, when the molten Cu comes in contact with solid Ni (melting point 1453 °C) a CuNi alloy can be formed. A melting temperature of copper-nickel alloy is between 1170 and 1240 °C depending on the Cu to Ni ratio. Higher melting point of cupronickel gives time for the densification and closing of the open porosity of alumina matrix. Hence, the leaking of molten metal is almost not observed. Low wettability of ceramics by molten metal, the flow of molten Cu through the pores of alumina matrix during the sintering as well as formation of CuNi alloy decrease the densification rate leading to some porosity in final samples [27–29].

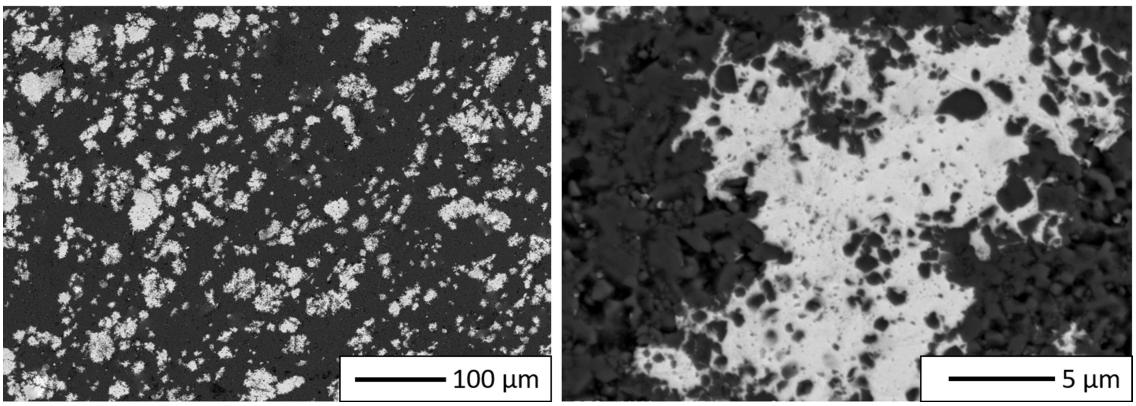

Figure 6. The micrographs of the polished cross section of the composites: metal particles are bright contrast, ceramics matrix is dark contrast

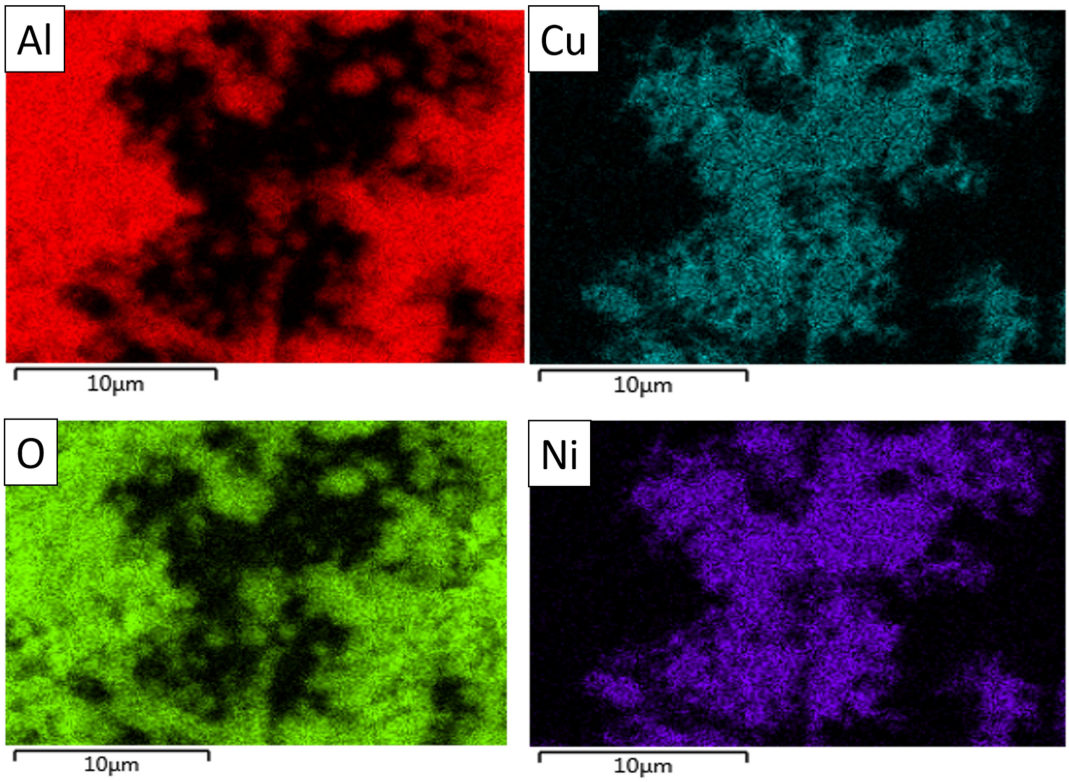

Figure 7. Analysis of the chemical composition for selected area on the polished cross section of Al_2O_3-Cu-Ni composites

Analysis of the particle size distribution of the metallic phase in composite (Fig. 8) obtained by the slip casting method revealed that more than 50% of particles have a diameter in the range of 15–21 µm. According to analyses of average diameter of metallic phase base powders, it can be concluded that composite preparation method has no influence on the average diameter of the metallic phases in the composite. The stereological analyses and the values of shape parameters reveal that the metal particles in the composite had the elongate and expanded shape. It was found that the curvature of grain boundary was equal to 1.28 ± 0.12, elongation was 1.55 ± 0.09 and the value of convexity was 1.12 ± 0.08 for the metal particles in Al_2O_3-Cu-Ni materials.

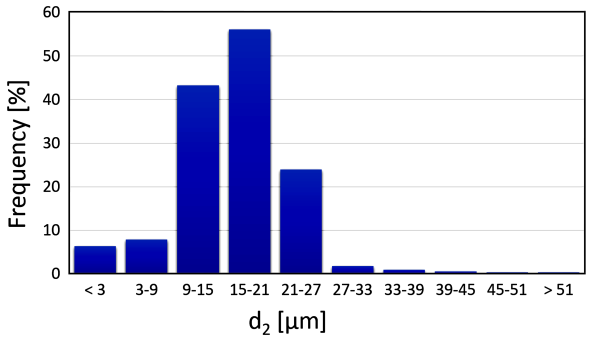

Figure 8. Particle size distribution of metallic phase in composite

The selected mechanical properties were shown in Table 1. The measurements showed that Vickers hardness for the composite is equal to 11.04 ± 0.5 GPa. The measurement also showed that the samples made

Table 1. Selected mechanical properties of specimens

Samples	*HV* [GPa]	K_{IC} (Niihara formula) [MPa · m$^{0.5}$]	K_{IC} (Anstis formula) [MPa · m$^{0.5}$]	Tensile strength (Brazilian test) [MPa]
Pure Al_2O_3	16.03 ± 0.3	4.97 ± 0.2	8.32 ± 0.9	223.21 ± 15
Al_2O_3-Cu-Ni	11.04 ± 0.5	6.17 ± 0.4	10.58 ± 1.2	62.40 ± 10

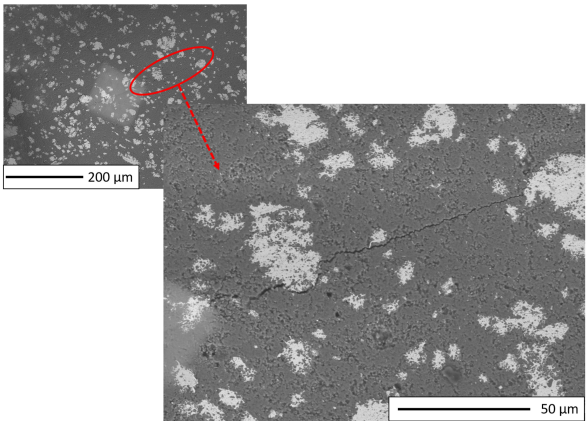

Figure 9. SEM microstructure of composites with marked examples of Vickers indentation in the sintered samples

from the pure Al_2O_3 had a hardness of 6.03 ± 0.3 GPa. In addition, it was found that similar results were obtained in Wiecińska's team for samples from pure alumina TM-DAR [30]. The observed higher hardness of the Al_2O_3-Cu-Ni composite for ca. 5 GPa in comparison to the pure alumina can be related to the presence of 15 vol.% of metal particles which show plastic deformation which increases hardness of such composite. The fracture toughness was determined using the Vickers indentation fracture toughness test with the use of two equations. Both equations (Eqs. 1 and 2) can be applied to median type of cracks. The K_{IC} values of the composite calculated on the basis of the Niihara and Anstis equations were 6.17 ± 0.4 and 10.58 ± 1.2, respectively. On the other hand, for the sample containing pure Al_2O_3 the K_{IC} values calculated on the basis of the Niihara and Anstis equations were 4.97 ± 0.2 and 8.32 ± 0.9, respectively. The addition of 15 vol.% of metal particles increased the fracture toughness for about 20% in comparison to the sample made from pure alumina TM-DAR. The mechanism of crack propagation is shown in Fig. 9. It was found that in the tested composites mechanism of crack propagation was crack deflection. Such a crack deflection mechanism creates a more sinuous route to release stress, which directly induces the increase in fracture toughness.

According to the literature data [31,32] the tensile strength of sintered alumina measured by Brasilian method should be around 243 MPa and 160 MPa for dynamic test and static test, respectively. Tensile strength of the pure Al_2O_3 sample prepared analogously like the composite is equal to 223.21±15 MPa. Due to the porosity, the tensile strength of the prepared composite sample was only 62.40 ± 10 MPa. Such result is rather low, especially as it was measured in dynamic conditions. It means that the conditions of sintering process should be improved to get better densification.

Fractography investigation was carried out to assess the mechanism of cracking in the obtained composite. SEM images in Fig. 10 show the fracture surface of the composite subjected to Brazilian test. Fractography analysis of the samples after fracture toughness test revealed that the bonds between the metallic particles and matrix are the weakest points of the composite. Observation of cracks between them allows to conclude that debonding of the particles and the matrix is main fracture mechanism of investigated composite. Additionally, the occurrance of craters in the matrix has been revealed. Observed craters have a bigger size than the pores identified in the composite before the Brazilian test which indicates that the craters on the fracture are residues of the pulled out particles from the ceramic matrix. The presence of the pulled out particles confirms weak adhesion of metal particles with the matrix.

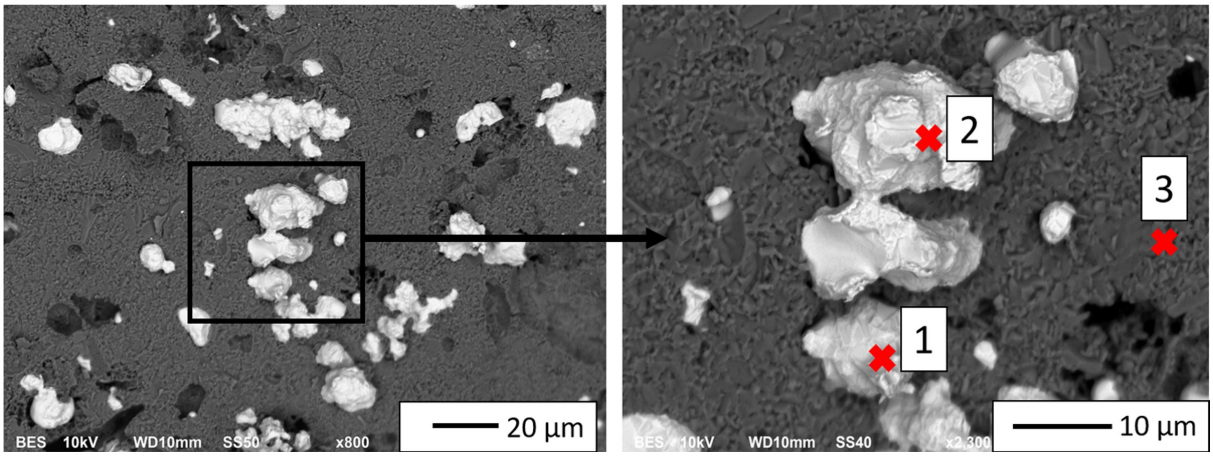

Figure 10. Examples of SEM images of the fracture surfaces of Al_2O_3-Cu-Ni composites

Table 2. EDX results of the composite at different measuring points presented in Fig. 10

Points	Weight [%]			
(Fig. 10)	O	Al	Ni	Cu
1	0.0 ± 0.0	0.0 ± 0.0	62.6 ± 0.5	37.4 ± 0.5
2	0.0 ± 0.0	0.0 ± 0.0	73.7 ± 0.5	26.3 ± 0.5
3	27.5 ± 0.2	72.5 ± 0.2	0.0 ± 0.0	0.0 ± 0.0

Additionally, point EDX analyses of the characteristic fracture areas were performed. Three measurements points are marked in Fig. 10 and corresponding concentrations of elements are shown in Table 2. The results of EDX measurements at points 1 and 2 revealed only nickel and copper in chemical composition of light metallic particles. It suggests that no chemical bonding was achieved during the sintering and only adhesion bonding was reached. Due to the lack of matrix residues on the particles it can be stated that the de-bonding of matrix/particle occurred by brittle cleavage. It confirms weak metallic phase/matrix adhesion. Lack of oxide in the results of measurements points 1 and 2 indicates also that the particles were not oxidized.

IV. Conclusions

It was found that the slip casting method can be used to obtain composites from Al_2O_3-Cu-Ni system. The X-ray diffraction patterns revealed the presence of Al_2O_3, Ni, Cu and CuNi solid solution phases. The studies indicate that the used reducting atmosphere used avoided the formation of spinel phases in the composite. Based on SEM, pores and voids are observed in the microstructure of obtained composite. Also, the distribution of elongated and expanded metallic particles in the matrix is homogeneous with the tendency for agglomeration. On the basis of the Brazilian test, fracture mechanism of the composite is related to cracking and de-bonding between ceramic matrix and metallic phase. The obtained results allow us to create a basic principle for controlling the microstructure and properties of ceramic matrix composites reinforced by metallic phase.

Acknowledgments: The study was accomplished thanks to the funds allotted by The National Science Centre within the framework of the research project 'OPUS 13' no. 2017/25/B/ST8/02036. This investigation is supported by the Foundation for Polish Science (FNP).

References

1. N. Travitzky, "Processing of ceramic–metal composites", *Adv. Appl. Ceram.*, **111** [5-6] (2012) 286–300.
2. F.J. Lino Alves, A.M. Baptista, A.T. Marques, "Metal and ceramic matrix composites in aerospace engineering", pp. 59–99, Ch. 3 in *Advanced Composite Materials for Aerospace Engineering: Processing, Properties and Applications*. Ed. S. Rana, R. Fangueiro, Woodhead Publishing, 2016.
3. K.H. Zum Gahr, *Microstructure and Wear of Materials*, Elsevier, 1987.
4. Y. Cao, J. Yan, N. Li, Y. Zheng, Ch. Xin, "Effects of brazing temperature on microstructure and mechanical performance of Al_2O_3/AgCuTi/Fe-Ni-Co brazed joints", *J. Alloys Compd.*, **650** (2015) 30–36.
5. H.M. Irshad, A.S. Hakeem, B.A. Ahmed, S. Ali, S. Ali, S. Ali, M.A. Ehsan, T. Laoui, "Effect of Ni content and Al_2O_3 particle size on the thermal and mechanical properties of Al_2O_3/Ni composites prepared by spark plasma sintering", *Int. J. Refract. Met. H.*, **76** (2018) 25–32.
6. M. Munro, "Evaluated material properties for a sintered alpha-alumina", *J. Am. Ceram. Soc.*, **80** [8] (2005) 1919–1928.
7. H.M. Irshad, A.A. Ahmed, M.A. Ehsan, T.I. Khan, T. Laoui, M.R. Yousaf, A. Ibrahim, A.S. Hakeem, "Investigation of the structural and mechanical properties of micro-/nano-sized Al_2O_3 and cBN composites prepared by spark plasma sintering", *Ceram. Int.*, **43** [14] (2017) 10645–10653.
8. M. Hasan, J. Zhao, Z. Jiang, "Micromanufacturing of composite materials: A review", *Int. J. Extrem. Manuf.*, **1** (2019) 012004.
9. B. Kafkaslioğlu Yildiz, H. Yilmaz, Y. Kemal Tur, "Processing and mechanical characterization of Al_2O_3/Ni and Al_2O_3/Co composites by pressureless sintering of nanocomposite powders", *Process. Appl. Ceram.*, **12** [2] (2018) 123–128.
10. A. Fathy, F. Shehata, M. Abdelhameed, M. Elmahdy, "Compressive and wear resistance of nanometric alumina reinforced copper matrix composites", *Mater. Design*, **36** (2012) 100–107.
11. R. Ritasalo, X.W. Liua, O. Soderberg, A. Keski-Honkola, V. Pitkanen, S.P. Hannula, "The microstructural effects on the mechanical and thermal properties of pulsed electric current sintered Cu-Al_2O_3 composites", *Procedia Eng.*, **10** (2011) 124–129.
12. X. Wang, S. Liang, P. Yang, Z. Fan, "Effect of Al_2O_3 content on electrical breakdown properties of Al_2O_3/Cu composite", *J. Mater. Eng. Perform.*, **19** [9] (2010) 1330–1336.
13. M. Ravikumar, H.N. Reddappa, R. Suresh, "Aluminium composites fabrication technique and effect of improvement in their mechanical properties – A review", *Mater. Today Proceed.*, **5** [11] (2018) 23796–23805.
14. G. Li, X. Huang, J. Guo, "Fabrication and mechanical properties of Al_2O_3-Ni composite from two different powder mixtures", *Mater. Sci. Eng. A*, **352** [1-2] (2003) 23–28.
15. K. Konopka, M. Maj, K.J. Kurzydłowski, "Studies of the effect of metal particles on the fracture toughness of ceramic matrix composites", *Mater. Charact.*, **51** [5] (2003) 335–340.
16. T. Rodriguez-Suarez, J.F. Bartolome, J.S. Moya, "Mechanical and tribological properties of ceramic/metal composites: A review of phenomena spanning from the nanometer to the micrometer length scale", *J. Eur. Ceram. Soc.*, **32** [15] (2012) 3887–3898.
17. J.A. Yeomans, "Ductile particle ceramic matrix composites – Scientific curiosities or engineering materials", *J. Eur. Ceram. Soc.*, **28** [7] (2008) 1543–1550.
18. M. Saralasrita, D. Bodhisatwa, D. Santanu, "Poly(maleic acid) – A novel dispersant for aqueous alumina slurry", *J. Asian. Ceram. Soc.*, **1** [2] (2013) 184–190.
19. J. Michalski, T. Wejrzanowski, R. Pielaszek, K. Konopka, W. Łojkowski, K.J. Kurzydłowski, "Application of image analysis for characterization of powders", *Mater. Sci. Poland*, **23** [1] (2005) 79–86.

20. K. Niihara, "A fracture mechanics analysis of indentation induced Palmqvist cracks in ceramics", *J. Mater. Sci.*, **2** [5] (1983) 221–223.
21. K. Niihara, R. Morena, D.P.H. Hasselmann, "Evaluation of K_{IC} of brittle solids by indentation method with low crack-to-indent ratios", *J. Mater. Sci.*, **1** [1] (1982) 13–16.
22. K. Strecker, S. Ribeiro, M.J. Hoffmann, "Fracture toughness measurements of LPSSiC: A comparison of the indentation technique and the SEVNB method", *Mater. Res.*, **8** [2] (2005) 121–124.
23. A. Nastic, A. Merati, M. Bielawski, M. Bolduc, O. Fakolujo, M. Nganbe, "Instrumented and Vickers indentation for the characterization of stiffness, hardness and toughness of zirconia toughened Al_2O_3 and SiC armor", *J. Mater. Sci. Technol.*, **31** [8] (2015) 773–783.
24. G.R. Anstis, P. Chantikul, B.R. Lawn, D.B. Marshall, "A critical evaluation of indentation techniques for measuring fracture toughness: I, Direct crack measurements", *J. Am. Cer. Soc.*, **64** [9] (1981) 533–538.
25. M.L. Scapin, L. Peroni, M. Avalle, "Dynamic Brazillian test for mechanical characterization of ceramic ballistic protection", *Shock Vib.*, **2017** (2017) 1–10.
26. ASTM C496/C496M-17, *Standard Test Method for Splitting Tensile Strength of Cylindrical Concrete Specimens*, ASTM International, West Conshohocken, PA, 2017.
27. E. Gorges, I. Egry, "The surface tension of copper-nickel alloys", *J. Mater. Sci.*, **30** [10] (1995) 2517–2520.
28. J. Schmitz, J. Brillo, I. Egry, "Surface tension of liquid Cu and anisotropy of its wetting of sapphire", *J. Mater. Sci.*, **45** [8] (2010) 2144–2149.
29. P.D. Ownby, J. Liu, "Surface energy of liquid copper and single-crystal sapphire and the wetting behaviour of copper on sapphire", *J. Adhes. Sci. Technol.*, **2** [1] (1988) 255–269.
30. P. Wiecińska, D. Kubica, E. Pietrzak, A. Sakowicz, N. Prokurat, A. Antosik, "Diacryloyl derivative of mannitol - Synthesis and application in gelcasting of Al_2O_3-ZrO_2 composites", *Arch. Metall. Mater.*, **63** [2] (2018) 859–865.
31. R.C. Yu, G. Ruiz, A. Pandolfi, "Numerical investigation on the dynamic behavior of advanced ceramics", *Eng. Fract. Mech.*, **71** [4-6] (2004) 897–911.
32. Y. Tan, D. Yang, Y. Sheng, "Study of polycrystalline Al_2O_3 machining cracks using discrete element method", *Int. J. Mach. Tool. Manu.*, **48** [9] (2008) 975–982.